

Dynamics of vortex defect formation in two dimensional Coulomb crystals

Michael Arnold*

*Centre for Complex Systems, Faculty of Engineering,
The University of Sydney, Sydney, NSW 2006, Australia.*

Ramil Nigmatullin†

*Center for Engineered Quantum Systems, Dept. of Physics & Astronomy, Macquarie University, 2109 NSW, Australia.
(Dated: May 21, 2022)*

We study the non-equilibrium dynamics of two dimensional planar ion Coulomb crystals undergoing a structural buckling transition to a three plane configuration, driven by a reduction of the transverse confining frequency. This phase transition can be theoretically modeled using a mapping to a two dimensional Ginzburg-Landau theory with complex order parameter field. We demonstrate that finite rate quenches result in creation of stable topological vortices, which are localized point regions around which the phase of the order parameter field winds a multiple of 2π . The density of the defects as a function of quench rate is investigated using molecular dynamics simulations and its scaling is shown to be consistent with Kibble-Zurek theory of defect formation. Following the quench, the annihilation of vortex and anti-vortex pairs results in the relaxation of defect density that follows a diffusive scaling with a logarithmic correction. This work highlights the potential for investigating complex non-equilibrium statistical physics of topological defects in an experimentally accessible ion trap setting.

I. INTRODUCTION

Trapped ions is one of the most prominent quantum technologies. Doppler laser cooling can bring ions to low temperatures at which the ions crystallize forming regular structures, known as Coulomb crystals, whose shape is determined by the trapping parameters. Linear chain crystals in Paul traps have the simplest phonon spectrum and have been widely used in metrology [1], quantum computing [2, 3] and quantum simulations [4]. In Penning traps, large two dimensional planar crystals can be readily created and these structures have also been used in metrology and quantum information processing applications [5].

Beyond these simple Coulomb crystal geometries, there is great interest in exploring more complex structural phases and the transitions between them. The strong long-range Coulomb interactions between particles leads to highly non-linear non-trivial dynamics, whose investigation is of fundamental interest in the fields of nonlinear science, complex systems and solid-state physics; it is useful as a platform for studying complex non-linear and non-equilibrium dynamics in areas including the simulation of Klein-Gordon fields on a lattice [6], Kibble-Zurek mechanism of defect formation [7–9], dynamics of discrete solitons [10, 11], dry friction [12], energy transport [13, 14] and synchronization [15]. Coulomb crystals with more complexity also provide new lattice geometries for quantum simulations [16].

In this paper, we investigate numerically the non-equilibrium structural phase transition from a quasi-two-dimensional 1-plane crystal to a 3-plane crystal. We fo-

cus on the Kibble-Zurek mechanism of the formation of topological defects and the subsequent coarsening dynamics of annihilation of defects and anti-defect pairs. Previous studies of KZ mechanism in ion crystal systems have focused on the linear to zigzag phase transition in a quasi-one-dimensional system [7, 8]. This is symmetry breaking phase transitions and the resulting defects are either kinks [7, 8] if the Z_2 symmetry is broken or helical twists [9] if the $U(1)$ symmetry is broken. The 1-plane to 3-plane structural phase transition considered in this paper can be described by an XY 6-clock model with an intermediate Kosterlitz-Thouless phase. The defects are $U(1)$ point vortices whose physics is considerably richer [17].

Previously, simulations of finite quenches in a two dimensional XY spin model have shown that the density of vortices is dictated by both the KZ mechanism and coarsening dynamics of annihilation of vortex/anti-vortex pairs [18]. This observation was corroborated in an experimental study of colloids undergoing a phase transition via Kosterlitz–Thouless–Halperin–Nelson–Young (KTHNY) melting scenario [19]. The molecular dynamics simulations of microscopic ion crystal dynamics presented in this paper are consistent with the dynamics observed in [18, 19]. An observed deviation from the theoretical coarsening scaling may be attributed to the pinning effect of the 6-clock potential. Our work introduces a new platform for investigating the non-equilibrium KT phase transition and more generally the collective dynamics of interacting vortices.

The paper is organized as follows. Section II presents the microscopic model, reviews its mapping to the Ginzburg-Landau field theory and the phase diagram of a 1-plane to 3-plane structural transition. Section III uses molecular dynamics simulations to demonstrate the existence of topological defects in the 3-plane phase and

* michael.arnold@sydney.edu.au

† ramil.nigmatullin@mq.edu

presents an algorithm for determining their location. Section IV focuses on molecular dynamics investigation of finite rate quenches, where the KZ mechanism and coarsening dictate the evolution of the average number of defects in the system.

II. GINZBURG-LANDAU MODEL OF 1- TO 3-PLANE TRANSITION

Ion traps confine repulsively interacting ions in space either by rapidly varying oscillatory electric fields, as in the Paul traps, or a combination of static electric and magnetic fields, as in the Penning traps [20]. The dynamics of ion Coulomb crystal can be often approximated with the so-called pondermotive approximation or pseudopotential theory, which replaces the time-varying trapping fields experienced by particles by an effective time-independent harmonic potential. The laser cooling reduces the temperature of the ions such that they can form regular crystal-like configurations, whose overall shape is determined by the trap parameters. We will consider a system of N ions confined to a periodic cell in the x - y plane and by the harmonic confinement in the z -direction. The potential energy is given by

$$V = \frac{1}{2}m\omega_z \sum_j z_j^2 + \mathcal{K} \sum_{i < j} \frac{1}{|\mathbf{r}_i - \mathbf{r}_j|} \quad (1)$$

where $\mathbf{r}_j = (x_j, y_j, z_j)$ are the coordinates of the j th ion, $\mathcal{K} \equiv q^2/4\pi\epsilon_0$, q is the charge of the ion, ϵ_0 is the vacuum permittivity, m is the mass of the ion and ω_z is the trapping frequency in the z -direction. The periodic boundary conditions results in a homogeneous spacing in the ion crystal. In a real experimental system, the open boundary conditions and the harmonic confinement in the x and y direction would result in inhomogeneous spacing between the ions; the ions are closer together in the centre of the crystal and further apart near the edges. The system with periodic boundary condition can be viewed as an approximation to a central region of a large ion crystal, where the spacing is approximately homogeneous and the boundary effects can be neglected.

Above a certain critical value of $\omega_z = \omega_z^{(c)}$ the lowest energy configuration is a planar triangular lattice. When the confining frequency is reduced to below $\omega_z^{(c)}$, the 1-planar crystal configuration undergoes a buckling structural transition into a 3-planes, all of which in triangular lattice geometry but with double the lattice spacing (see Figure 1). This buckling instability has been predicted in an early theoretical work by Dubin [21] and has been observed experimentally in [22]. Recently, Podolsky *et al.* [17] derived a Ginzburg-Landau (GL) field theory for this transition thereby proving that it is in the universal class of a two dimensional XY model [17].

The GL field theory is derived by Taylor expanding the non-linear Coulomb interaction term in equation (1) in

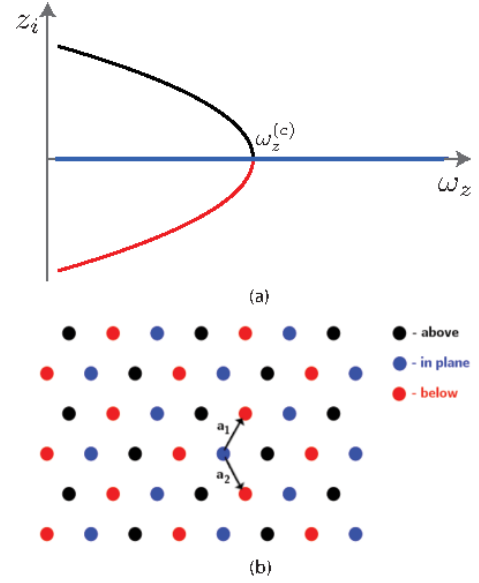


FIG. 1. Structural buckling transition between a 1-plane and 3-plane configuration. (a) The transverse displacement of the ions in a crystal at different values of ω_z in the vicinity of the critical $\omega_z^{(c)}$. (b) The triangular lattice structure of the 3-plane phase.

displacements around the equilibrium lattice positions. In [17] it was shown that one must keep the terms up to the sixth order in the expansion to correctly capture the critical properties of the structural phase transition. The GL free energy density is given by

$$\frac{f}{\mathcal{K}} = \frac{\gamma}{2} |\nabla\psi|^2 + \epsilon |\psi|^2 + u |\psi|^4 + v |\psi|^6 + \frac{w}{2} [\psi^6 + (\psi^*)^6] \quad (2)$$

where $\epsilon = \frac{1}{\sqrt{3}} \left(\frac{m\omega_z^2 a^2}{2\mathcal{K}} - I_2 \right)$, $u = 3/\sqrt{3}/4I_4$, $w = \frac{5}{8\sqrt{3}}I_6$, $v = -\frac{25}{4\sqrt{3}}I_6$, $I_2 = 6.683$, $I_4 = 3.56$, $\gamma = 0.223$, $I_6 = 2.558$ and a is the lattice spacing. The order parameter field at a lattice point with coordinates $(x_j, y_j, \psi(x_j, y_j))$, is an implicit function of the transverse displacement

$$z_j = \text{Re} [\psi e^{i\mathbf{K} \cdot \mathbf{r}_j}]. \quad (3)$$

Here \mathbf{K} is the base vectors of the first Brillouin zone of the triangular lattice given by $\mathbf{K} = (4\pi/3, 0)$, $\mathbf{r}_i = n_1 \mathbf{a}_1 + n_2 \mathbf{a}_2$, with $\mathbf{r}_{1,2} = (\frac{1}{2}, \pm\sqrt{3}/2)$. The order parameters ψ is complex and can be expressed as $\psi = |\psi|e^{i\theta}$.

The potential energy for the mean field configuration, which neglects the spatial fluctuations in the order parameter, $V(\psi)/\mathcal{K} = \epsilon |\psi|^2 + u |\psi|^4 + v |\psi|^6 + \frac{w}{2} [\psi^6 + (\psi^*)^6]$, is shown in Figure 2. For $\epsilon > 0$ the order parameter is zero, $\psi = 0$, and the system is in the 1-plane phase. The potential is a single well and since the order parameter has no preferred direction, the 1-plane phase is disordered. For $\epsilon < 0$ the order parameter is non-zero and the system is in the 3-plane phase. The potential

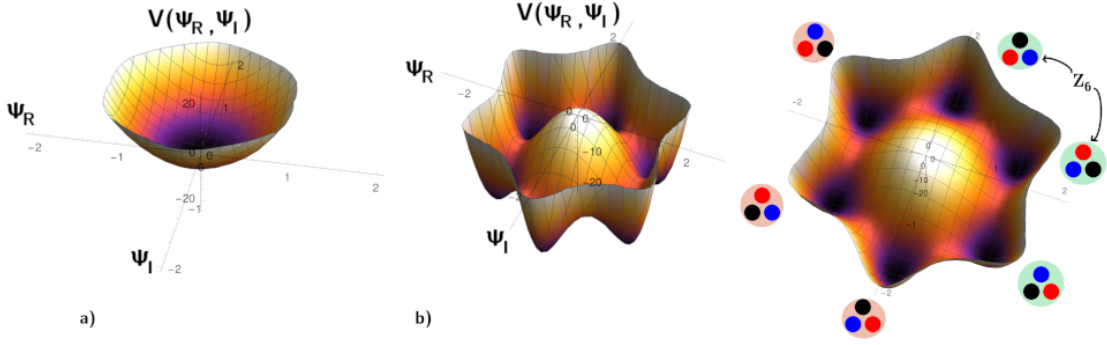


FIG. 2. (a) Single well potential of GL theory for $\epsilon > 0$ (b) Mexican hat potential for $\epsilon < 0$.

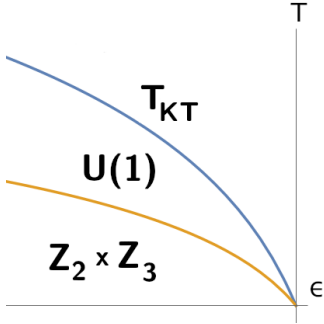


FIG. 3. Phase Diagram of a Coulomb Crystal in parameter space with respect to temperature T and the coefficient ϵ .

is a Mexican hat but with 6 equally spaced wells which correspond to the local order of the 6 degenerate lattice arrangements shown in Figure 2(b). This corresponds to the 6-clock phase which has the discrete $Z_2 \times Z_3$ symmetry. At higher energies the order parameter can easily overcome the energy barrier between the neighboring minima, and the symmetry changes to $U(1)$ continuous symmetry. Two dimensional systems with the $U(1)$ symmetry in the order parameters support topological defect vortex configuration, which are localized regions where the field winds around the Mexican hat potential. The presence of these topological defects drastically alters the physics of the system leading to the existence of the KT phase [23, 24]. Thus, near the critical point of the 1-plane to 3-plane structural phase transition the system can exist in 3 phases, disordered, KT and the 6-face clock phases, depending on the value of ϵ and temperature T . The phase diagram was derived in [17] and is sketched in Figure 3. The KT phase is characterized by a change in behavior in correlation length. For $T > T_{KT}$, the system is disordered, the correlation length decays exponentially and there is a finite density of unbound vortices. For $T < T_{KT}$, there is a quasi-long range order with a power law decays of the correlation length and vortices and anti-vortices form bound pairs. For $T < T^*$, the system is in the 6-clock phase, which again exhibits a long-range order with exponentially decaying correlation length.

III. TOPOLOGICAL DEFECTS IN THE 3-PLANE PHASE

To verify the prediction of the existence of the topological defects, we have performed molecular dynamics simulations of ion Coulomb crystals confined in a box with periodic boundary conditions in the x and y direction. The topological defects are produced by quenching a system from a 1-plane disordered phase into the 3-plane phase. We use a Langevin thermostat to simulate the interaction of the ions with the cooling laser beam, which thermalized the ions. The equations of motion for the j th ion are given by

$$m\partial_{tt}x_j = -m\gamma\partial_t x_j - \partial_{x_j} V_c + \theta_{xj}(t) \quad (4)$$

$$m\partial_{tt}y_j = -m\gamma\partial_t y_j - \partial_{y_j} V_c + \theta_{yj}(t) \quad (5)$$

$$m\partial_{tt}z_j = -m\omega(t)^2 - m\gamma\partial_t z_j - \partial_{z_j} V_c + \theta_{zj}(t), \quad (6)$$

where m is the mass of the ion, $\omega(t)$ is the transverse confining frequency, V_c is the Coulomb interaction energy, γ is the friction coefficient. The force $(\theta_{xj}, \theta_{yj}, \theta_{zj})$ is the stochastic thermal force satisfying $\langle \theta_{\alpha,j}(t) \rangle = 0$ and $\langle \theta_{\alpha,j}(t)\theta_{\beta,k}(t') \rangle = 2m\gamma k_B T \delta_{\alpha\beta} \delta_{jk} \delta(t-t')$, where $\langle \dots \rangle$ denotes ensemble averaging. The integration of the equation of motion is performed using GPU accelerated OpenMM [25] framework, and Ewald sums are used to approximate the Coulomb interactions in the x and y directions.

To determine the location of defects in a given ion crystal configuration, one must compute the local order parameter field ψ using the individual ion coordinates. Using equation (3) the order parameter in the 6-clock phase can be written as

$$z_i = \text{Re}[\Psi e^{\mathbf{K} \cdot \mathbf{r}_i}] \quad (7)$$

$$= |\psi| \cos\left(\frac{\pi(2n_i + 1)}{6} + \delta\Theta_i + \mathbf{K} \cdot \mathbf{r}_i\right), \quad (8)$$

where $n_i \in \{1, \dots, 6\}$ determines the clock state at the position of the i th ion and $\delta\Theta_i$ is the fluctuation about this phase. Denoting the splitting between the planes as $h \equiv \max_i(|\langle z_i \rangle|)$, where z_i is the z -coordinate of an

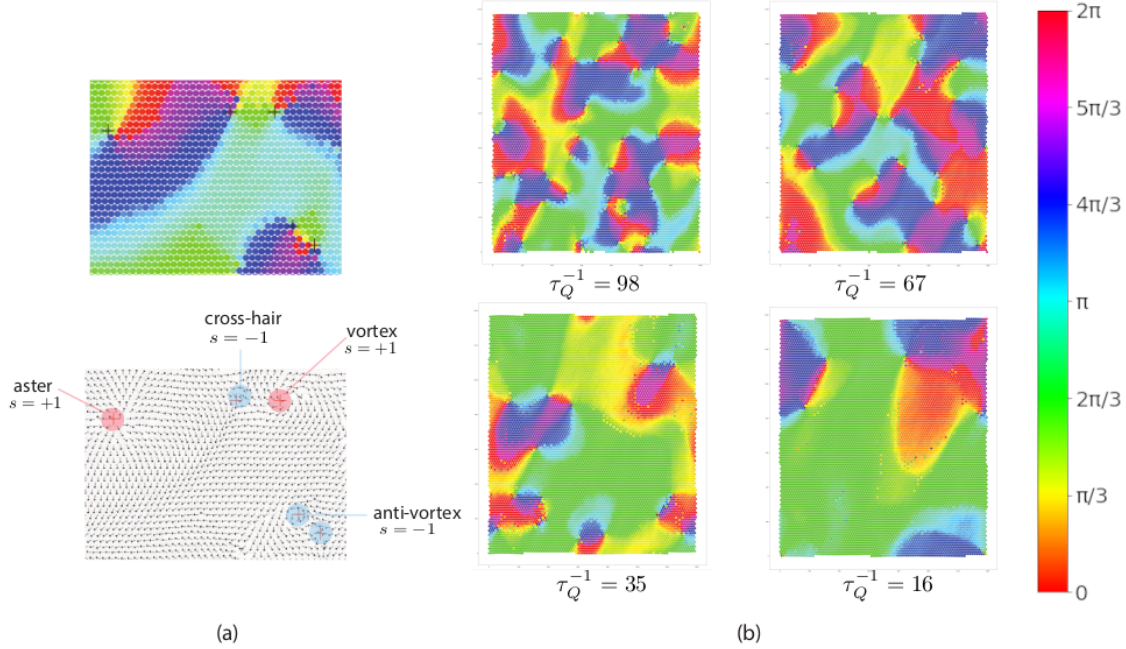


FIG. 4. a) Examples of a configuration with topological defects in the 3-plane structural phase represented as color plot (top) or arrow plot (bottom). The observed defects are asters and vortices (topological charge, $s = +1$) or cross-hairs and anti-vortices (topological charge, $s = -1$) (b) Instantaneous configurations of a quasi-two-dimensional ion crystal with 9858 Be^+ ions at a temperature of $20\mu\text{K}$ and $\gamma = 8.96 \times 10^{-7} \text{ps}^{-1}$ in the 3-plane structural phase at the end of a non-equilibrium quench from a disordered single plane phase at different rate τ_Q^{-1} . The quench is implemented by reducing the transverse confining frequency ω_z . The density of topological defects increases with increasing quench rate. Each color corresponds to a phase angle Θ of the local order parameter $\psi = |\psi|e^{i\Theta}$.

ion either in the $+$ or $-$ sublattice of the 3-plane structural phase, one finds that $h = |\psi| \cos(\pi/6) \langle \cos(\delta\Theta) \rangle$ and equation (8) can be written as

$$z_i = \frac{h}{\cos(\pi/6)} \cos \left(\delta\Theta_i + \frac{\pi(2n_i + 1)}{6} + \mathbf{K} \cdot \mathbf{r}_i \right). \quad (9)$$

The values of clock state at each point, n_i , are determined by allocating a phase value to an arbitrary chosen patch of three adjacent ions and then assigning all other patches the best matching value relative to this chosen reference. After assigning n_i , the correction term, $\delta\Theta_i$, is obtained by solving numerically the non-linear equation (9) using gradient descent algorithm.

Figure 4(a) shows a typical configuration with topological defects. The locations of the defects are determined by finding localized regions on the boundary of which the phase Θ winds an integer multiple of 2π . The topological charge s of a defect is defined as a winding number along the contour C encircling the defect i.e. $s = \frac{1}{2\pi} \int_C \partial_l \Theta dl$ where l is the position along the path of the chosen contour. In our simulations, we observe 4 types of point defects: asters and vortices with charge $+1$, and cross-hairs and anti-vortices with charge -1 . The existence of such defects may be predicted on general homotopy theoretic arguments [26]. Here, we have demonstrated that

in 3-plane Coulomb crystal all four types of defects are energetically stable.

The crystal configuration shown in the Figure 4(a) is in the 6-face clock phase rather than the KT phase, as there are clear boundary lines between the domains separating the regions with phase angles of the possible minimum energy configuration. Increasing the temperature in the system blurs the boundary lines until the system reaches a KT phase, where there is no energetically preferred phase angles Θ . In the KT phase there is no long-range order in the system - the defects are mobile and oppositely charged defects tend to annihilate. The long range order established by entering the clock phase and the energy of the Z_6 domain walls, appears to have a stabilizing effect on the point defects, reducing significantly their mobility.

IV. KIBBLE-ZUREK MECHANISM OF DEFECT FORMATION

Quenching the system from a disordered phase into the ordered phase at different rates results in different defect densities as can be seen in Figure 4(b). The relationship between the number of defects and the quench rates across symmetry breaking phase transitions was initially investigated by Kibble in the context of cosmology [27]

and Zurek in the context of condensed matter [28], in what became known as Kibble-Zurek (KZ) theory. Experimentally, the KZ mechanism for a 6-clock model has been investigated in the context of ferroelectric materials [29, 30]. One should note, however, that in ferroelectrics the transition happens in three dimensions where there is no KT phenomena.

Lets review the KZ mechanism as applied to continuous second order phase transitions. Consider approaching the critical point of a symmetry breaking second order phase transition. The correlation length ξ , defined by $\langle \psi(0, t) \psi(r, t) \rangle \sim e^{-r/\xi}$, diverges as a power law of the control parameter $\xi = \xi_0/|\epsilon|^\mu$, where μ is the critical exponent. The system also slows down on the approach to the critical point i.e. the relaxation time, τ , defined as $\langle \psi(0) \psi(t) \rangle \sim e^{-t/\tau}$ diverges as $\tau = \tau_0/|\epsilon|^\mu$. KZ mechanism proposes that the correlation length freezes out when the relaxation time is equal to the time left until the crossing of the point i.e. the freeze out time \hat{t} is found by solving $\tau(\hat{t}) = \tau_Q$. This “cross-over” time \hat{t} marks a transition between the adiabatic dynamical regime, where the correlation lengths adjust to its equilibrium value, and impulsive regime, where the correlation length is fixed. For a linear quench $\epsilon = t/\tau_Q$, one observes $\hat{t} = (\tau_0 \tau_Q^\mu)^{1/(1+\mu)}$ and the freeze-out correlation length is $\hat{\xi} = \xi(\hat{t}) = \xi_0(\tau_q/\tau_0)^{\nu/(1+\mu)}$. In the two dimensional system, the number of defects n is inversely proportional to the square of the correlation length scale in the system i.e. $n \propto \xi^{-2}$. Thus, the KZ prediction for the defect density in the end of the quench is $n_f = \hat{\xi}^{-2} \sim (\tau_q/\tau_0)^{-2\nu/(1+\mu)}$.

For KT phase transition, the same arguments applies except the correlation length diverge exponentially at the critical point rather than algebraically i.e. $\xi \sim \exp(a|\epsilon|^{-\mu})$ and $\tau \sim \exp(b|\epsilon|^{-\nu})$, where ϵ . In this case, the equation for the freeze-out time, $\hat{t} = \tau_Q$ cannot be solved exactly, but can still be determined numerically [18, 19]. An additional complication is that the generated vortex defects can be highly mobile and the process of annihilation of defects with opposite topological charges leads to the growth of correlation length in the system. Thus, the number of defects in the “impulsive” regime is not fixed but continuously decreases as the defects annihilate. In the context of sudden quenches, this growth of correlation length is known as coarsening.

In [18, 31], the authors propose that for a quench into the KT phase, one should account for both KZ mechanism and coarsening expressing the time evolution of correlation length as

$$\xi(t) = \begin{cases} \xi_{eq}(t), & \text{for } t < \hat{t} \\ \hat{\xi} + f(t), & \text{for } t \geq \hat{t} \end{cases}, \quad (10)$$

where $f(t)$ is the function representing the growth of the correlation length due to coarsening. Equation (10) expresses the idea that before the KZ freeze-out time, \hat{t} , the correlation length adopts its thermal equilibrium

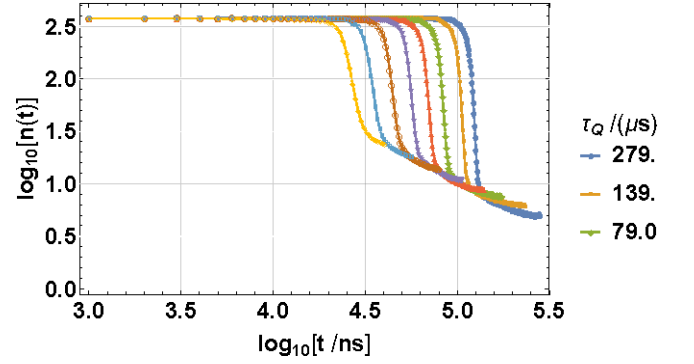


FIG. 5. Evolution of the average number of defects following quenches from 1-plane disordered phase into a 3-lane 6 face clock phase at finite rate $1/\tau_Q$. The simulated system contained 9858 Be^+ ions at a temperature of $20\mu\text{K}$ and $\gamma = 8.96 \times 10^{-7} \text{ps}^{-1}$ confined in a periodic box in the xy directions of size $1395.00 \times 1376.98 \mu\text{m}$. The starting and ending frequencies were set to $\omega_z^{(i)} = 7.70 \text{ Mhz}$ and $\omega_z^{(f)} = 7.42 \text{ Mhz}$, and the critical frequency is $\omega_z^{(i)} = 7.60 \text{ Mhz}$.

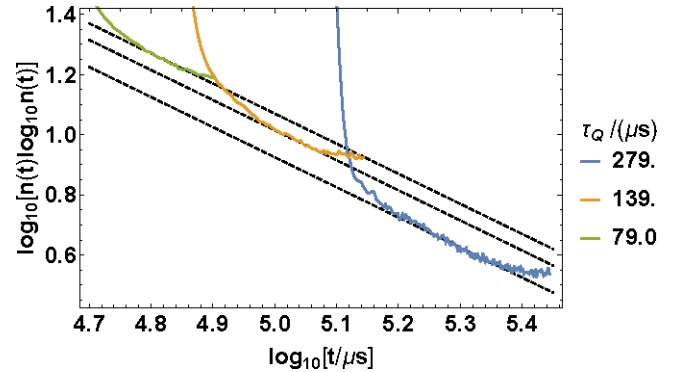


FIG. 6. Late time evolution of the average number of defects for three quenches at different rates $1/\tau_Q$. The slopes of the dashed lines is -1, indicating a $n \ln n \sim t^{-1}$ coarsening scaling.

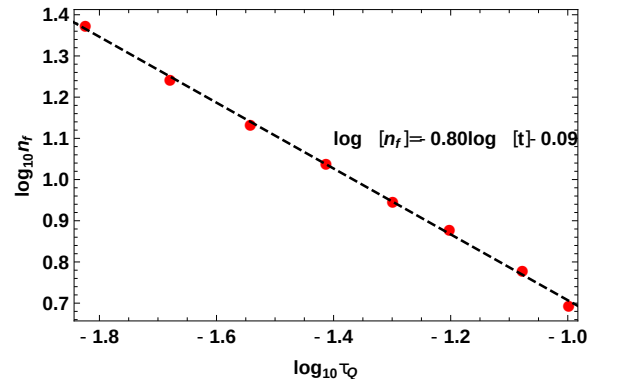


FIG. 7. Plot of the number of defects at the end of the quench, n_f as a function of quench rates.

value, and after crossing \hat{t} the correlation length is growing via coarsening. In a two dimensional system, which is quenched from disordered into ordered phase in the presence of linear damping, one expects the coarsening to proceed via diffusing law, where the correlation length grows as the square root of time $f(t) \sim t^{1/2}$ [32]. Several studies noted that the approach to diffusive law can be slow and that the coarsening is more accurately described by including a logarithmic correction, $f(t) \sim (t/\ln t)^{1/2}$ [33, 34].

In [18], a good agreement between the analytic expression (10) and the numerical simulations of quenches in a two dimensional XY model is found. We have carried out molecular dynamics simulations to verify whether the dynamically crossing the 1-plane to 3-plane structural transition will result in the same defect scaling behavior. We simulate the dynamics of $N = 9858 Be^+$ ions at a temperature of $20\mu K$ and $\gamma = 8.96 \times 10^{-7} ps^{-1}$ confined to a periodic box in an xy directions and a harmonic potential in the z directions by numerically integrating equation (4)-(6). The system is first thermalized at a confinement frequency $\omega_z^{(i)}$ sufficiently far from the critical frequency $\omega_z^{(c)}$ such that the correlation length is small i.e. of the order of the lattice spacing. After that the confining frequency is decreased linearly at a rate, $\omega_z = \omega_z^{(i)} + t(\omega_z^{(f)} - \omega_z^{(i)})/\tau_Q$, such that the system undergoes a transition between a 1-plane and 3-plane structural phases at a rate $1/\tau_Q$. The defects are counted using the method presented in Section III, and in order to obtain the ensemble averaged defect number $\langle n(t) \rangle$ the simulations are carried out ~ 140 times for each τ_Q .

Figure 5 shows the evolution of the defect density as function of time following phase transition at different quench rates. Several dynamical regimes can be seen in the figure. Initially, the system is in the 1-plane phase far from phase transition point, the correlation length is small and the density of defects is large. As ω_z approaches the critical frequency, the defect density decreases adjusting to the new equilibrium values. This regime crosses over to rapid relaxation, where the density of vortices decreases significantly. According to the KZ theory, the crossover occurs at $t > \hat{t}$. The relaxation continues at a slower pace consistent with the power-law coarsening dynamics. Finally, the relaxation slows further as the system enters the clock phase and the domains are stabilized.

In Figure 6 we zoom in into the late time evolution at three different quench rates to verify whether the relaxation in the system is due to coarsening. The growth of the correlation length due to coarsening in the KT phase is predicted to follow $\xi \sim (t \ln t)^{1/2}$ and consequently the number of defects follow a powerlaw with a logarithmic

correction $n \ln n \sim t^{-1}$ [33]. In Figure 6, one can see that there is a region where the powerlaw with the logarithmic correction is valid. However, this regime crosses over fairly quickly to a regime of slower relaxation, which we believe is either due to the stabilizing effect of entering into the clock phase or the pinning of the vortices by the discreteness of the lattice.

Finally, Figure 7 shows the number of defects at the end of the quench at $t = \tau_Q$ as a function of τ_Q . We observe a powerlaw scaling with an exponent of -0.80 i.e. $n(t = \tau_Q) \propto \tau_Q^{-0.80}$. While an accurate determination of the KZ scaling law involves numerical estimation of \hat{t} , previous simulation results for quenches of the two dimensional XY spin model found a powerlaw scaling of -0.72 at intermediate values of τ_Q . The exponent of -0.80 observed in our simulations is consistent with these previous findings.

V. CONCLUSION

In this paper we have studied the non-equilibrium dynamics of a planar Coulomb crystals undergoing a structural transition from a 1-planar to 3-planar configurations. The mapping to the Ginzburg-Landau theory reveals that this phase transition corresponds to a transition from a disordered paramagnetic phase to an ordered 6-clock phase with an intermediate KT phase. We used molecular dynamics simulations to confirm that the KT and the 6-clock phase support stable topological defect structures: vortices, anti-vortices, cross-hairs and asters. The density of defects depends on the quench rate of the structural transition as predicted by the Kibble-Zurek theory of defect formation. We have verified that the defect scaling law is consistent with KZ scaling previously observed in numerical simulation of two dimensional XY spin model. Moreover, we have observed signatures of coarsening due to defect/anti-defect annihilation, which follows a relaxation powerlaw with a logarithmic correction.

Our work demonstrates that large planar ion Coulomb crystals can be used as model for studying non-equilibrium statistical physics of vortices in an effectively quasi-two-dimensional system. Such Coulomb crystals with open boundary conditions can be realized in Penning traps. While the focus of this paper was on the system with repulsive Coulomb interactions, similar transition is expected for a lattice with dipolar interactions [17]. We hope that our work will stimulate research towards experimental study of the predicted topological defects and their rich collective dynamics.

[1] J. Keller, D. Kalincev, T. Burgermeister, A. P. Kulosa, A. Didier, T. Nordmann, J. Kiethe, and T. Mehlstäubler,

Probing time dilation in coulomb crystals in a high-precision ion trap, Phys. Rev. Applied **11**, 011002 (2019).

- [2] H. Häffner, C. Roos, and R. Blatt, Quantum computing with trapped ions, *Physics Reports* **469**, 155 (2008).
- [3] C. D. Bruzewicz, J. Chiaverini, R. McConnell, and J. M. Sage, Trapped-ion quantum computing: Progress and challenges, *Applied Physics Reviews* **6**, 021314 (2019), <https://doi.org/10.1063/1.5088164>.
- [4] K. Kim, M.-S. Chang, S. Korenblit, R. Islam, E. E. Edwards, J. K. Freericks, G.-D. Lin, L.-M. Duan, and C. Monroe, Quantum simulation of frustrated ising spins with trapped ions, *Nature* **465**, 590 (2010).
- [5] J. W. Britton, B. C. Sawyer, A. C. Keith, C.-C. J. Wang, J. K. Freericks, H. Uys, M. J. Biercuk, and J. J. Bollinger, Engineered two-dimensional ising interactions in a trapped-ion quantum simulator with hundreds of spins, *Nature* **484**, 489 (2012).
- [6] A. Retzker, R. C. Thompson, D. M. Segal, and M. B. Plenio, Double well potentials and quantum phase transitions in ion traps, *Phys. Rev. Lett.* **101**, 260504 (2008).
- [7] K. Pyka, J. Keller, H. L. Partner, R. Nigmatullin, T. Burgermeister, D. M. Meier, K. Kuhlmann, A. Retzker, M. B. Plenio, W. H. Zurek, A. del Campo, and T. E. Mehlstäubler, Topological defect formation and spontaneous symmetry breaking in ion coulomb crystals, *Nature Communications* **4**, 2291 (2013).
- [8] S. Ulm, J. Roßnagel, G. Jacob, C. Degünther, S. T. Dawkins, U. G. Poschinger, R. Nigmatullin, A. Retzker, M. B. Plenio, F. Schmidt-Kaler, and K. Singer, Observation of the kibble-zurek scaling law for defect formation in ion crystals, *Nature Communications* **4**, 2290 (2013).
- [9] R. Nigmatullin, A. del Campo, G. De Chiara, G. Morigi, M. B. Plenio, and A. Retzker, Formation of helical ion chains, *Phys. Rev. B* **93**, 014106 (2016).
- [10] H. L. Partner, R. Nigmatullin, T. Burgermeister, K. Pyka, J. Keller, A. Retzker, M. B. Plenio, and T. E. Mehlstäubler, Dynamics of topological defects in ion coulomb crystals, *New Journal of Physics* **15**, 103013 (2013).
- [11] H. Landa, B. Reznik, J. Brox, M. Mielenz, and T. Schaetz, Structure, dynamics and bifurcations of discrete solitons in trapped ion crystals, *New Journal of Physics* **15**, 093003 (2013).
- [12] J. Kiethe, R. Nigmatullin, D. Kalincev, T. Schmirander, and T. E. Mehlstäubler, Probing nanofriction and aubry-type signatures in a finite self-organized system, *Nature Communications* **8**, 15364 (2017).
- [13] T. Pruttivarasin, M. Ramm, I. Talukdar, A. Kreuter, and H. Häffner, Trapped ions in optical lattices for probing oscillator chain models, *New Journal of Physics* **13**, 075012 (2011).
- [14] L. Timm, H. Weimer, L. Santos, and T. E. Mehlstäubler, Energy localization in an atomic chain with a topological soliton, *Phys. Rev. Research* **2**, 033198 (2020).
- [15] T. E. Lee and M. C. Cross, Pattern formation with trapped ions, *Phys. Rev. Lett.* **106**, 143001 (2011).
- [16] A. Bermudez, J. Almeida, F. Schmidt-Kaler, A. Retzker, and M. B. Plenio, Frustrated quantum spin models with cold coulomb crystals, *Phys. Rev. Lett.* **107**, 207209 (2011).
- [17] D. Podolsky, E. Shimshoni, G. Morigi, and S. Fishman, Buckling transitions and clock order of two-dimensional coulomb crystals, *Phys. Rev. X* **6**, 031025 (2016).
- [18] J. Asja and F. C. Leticia, Quench dynamics of the 2d xy model, *J. Stat. Mech.* (2011).
- [19] S. Deutschländer, P. Dillmann, G. Maret, and P. Keim, Kibble-zurek mechanism in colloidal monolayers, *Proc Natl Acad Sci USA* **112**, 6925 (2015).
- [20] P. K. Gosh, *Ion Traps* (Clarendon Press, Oxford, 1995).
- [21] D. H. E. Dubin, Theory of structural phase transitions in a trapped coulomb crystal, *Phys. Rev. Lett.* **71**, 2753 (1993).
- [22] T. B. Mitchell, J. J. Bollinger, D. H. E. Dubin, X.-P. Huang, W. M. Itano, and R. H. Baughman, Direct observations of structural phase transitions in planar crystallized ion plasmas, *Science* **282**, 1290 (1998), <https://science.sciencemag.org/content/282/5392/1290.full.pdf>.
- [23] V. L. Berezinsky, Destruction of long range order in one-dimensional and two-dimensional systems having a continuous symmetry group. I. Classical systems, *Sov. Phys. JETP* **32**, 493 (1971).
- [24] J. M. Kosterlitz and D. J. Thouless, Ordering, metastability and phase transitions in two-dimensional systems, *Journal of Physics C: Solid State Physics* **6**, 1181 (1973).
- [25] P. Eastman, J. Swails, J. D. Chodera, R. T. McGibbon, Y. Zhao, K. A. Beauchamp, L.-P. Wang, A. C. Simmonett, M. P. Harrigan, C. D. Stern, R. P. Wiewiora, B. R. Brooks, and V. S. Pande, Openmm 7: Rapid development of high performance algorithms for molecular dynamics, *PLOS Computational Biology* **13**, 1 (2017).
- [26] N. D. Mermin, The topological theory of defects in ordered media, *Rev. Mod. Phys.* **51**, 591 (1979).
- [27] T. Kibble, Some implications of a cosmological phase transition, *Physics Reports* **67**, 183 (1980).
- [28] W. H. Zurek, Cosmological experiments in superfluid helium?, *Nature* **317**, 505 (1985).
- [29] S. M. Griffin, M. Lilienblum, K. T. Delaney, Y. Kumagai, M. Fiebig, and N. A. Spaldin, Scaling behavior and beyond equilibrium in the hexagonal manganites, *Phys. Rev. X* **2**, 041022 (2012).
- [30] S.-Z. Lin, X. Wang, Y. Kamiya, G.-W. Chern, F. Fan, D. Fan, B. Casas, Y. Liu, V. Kiryukhin, W. H. Zurek, C. D. Batista, and S.-W. Cheong, Topological defects as relics of emergent continuous symmetry and higgs condensation of disorder in ferroelectrics, *Nature Physics* **10**, 970 (2014).
- [31] G. Biroli, L. F. Cugliandolo, and A. Sicilia, Kibble-zurek mechanism and infinitely slow annealing through critical points, *Phys. Rev. E* **81**, 050101 (2010).
- [32] M. Mondello and N. Goldenfeld, Scaling and vortex dynamics after the quench of a system with a continuous symmetry, *Phys. Rev. A* **42**, 5865 (1990).
- [33] B. Yurke, A. N. Pargellis, T. Kovacs, and D. A. Huse, Coarsening dynamics of the xy model, *Phys. Rev. E* **47**, 1525 (1993).
- [34] A. J. Bray, A. J. Briant, and D. K. Jervis, Breakdown of scaling in the nonequilibrium critical dynamics of the two-dimensional XY model, *Phys. Rev. Lett.* **84**, 1503 (2000).